

Supplementary Materials: Protease-Triggered Release of Stabilized CXCL12 From Coated Scaffolds in an Ex Vivo Wound Model

Sabrina Spiller, Tom Wippold, Kathrin Bellmann-Sickert, Sandra Franz, Anja Saalbach, Ulf Andreegg and Annette G. Beck-Sickinger

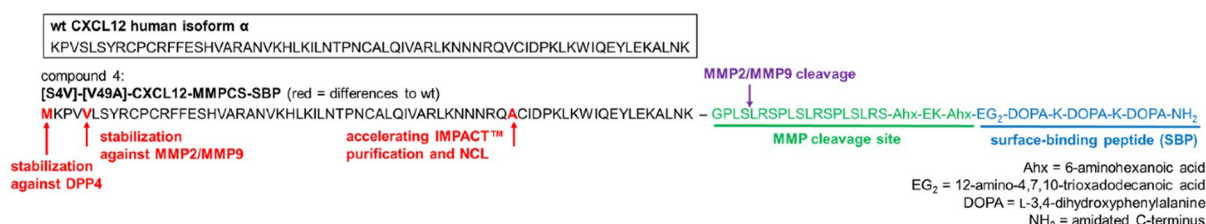


Figure S1. Sequence of wild type CXCL12 as well as introduced modifications and properties of compound 4.

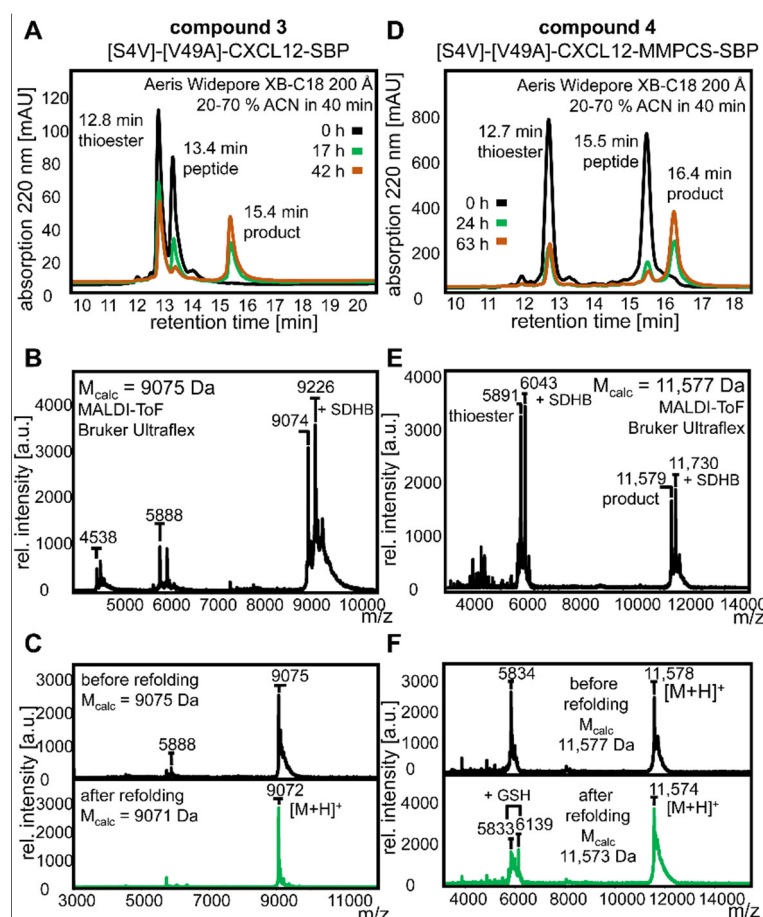


Figure S2. Analytics of NCL and refolding exemplarily for compound 3 (left) and compound 4 (right). (A+D) NCL was monitored during reaction by analytical RP-HPLC on a Phenomenex Aeris Widepore XB-C18 column (200 Å) using linear gradients of 0.1% TFA/H₂O and 0.08% TFA/ACN as indicated. (B+E) Identity of the product after NCL was proven by MALDI-ToF MS. (C+F) Successful refolding was verified by MALDI-ToF MS, showing a mass difference of m/z -4. GSH = glutathione, SDHB = super-dihydroxybenzoic acid matrix substance (m/z +152), M_{calc} = calculated molecular weight, ACN = acetonitrile.

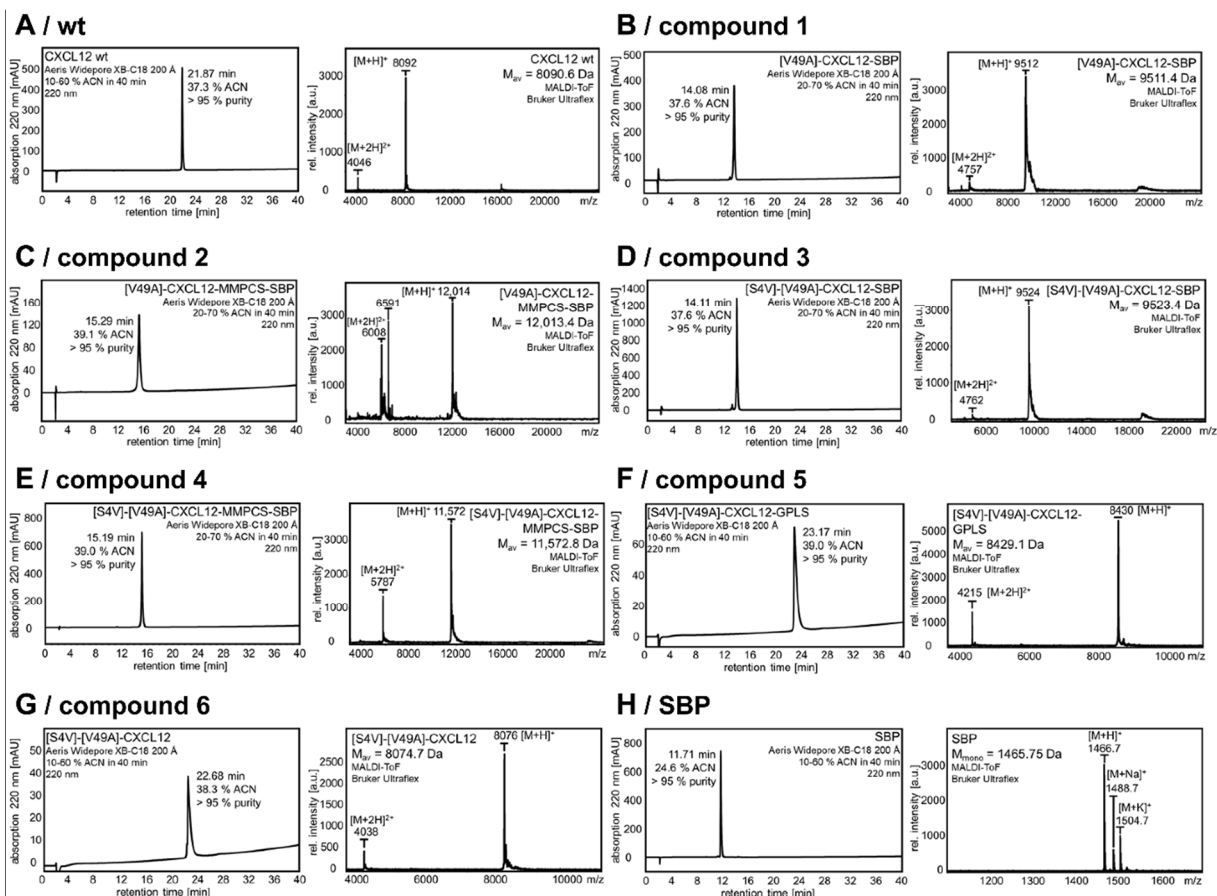


Figure S3. Analytics of generated compounds. Analytical RP-HPLC (left) was done on a Phenomenex Aeris Widepore XB-C18 column (200 Å) using linear gradients of 0.1% TFA/H₂O and 0.08% TFA/ACN as indicated. Identity was proven by MALDI-ToF MS (right). Analysis was done for (A) CXCL12 wt, (B) compound 1 ([V49A]-CXCL12-SBP(Biotin)), (C) compound 2 ([V49A]-CXCL12-MMPCS-SBP(Biotin)), (D) compound 3 ([S4V]-[V49A]-CXCL12-SBP, (E) compound 4 ([S4V]-[V49A]-CXCL12-MMPCS-SBP, (F) compound 5 ([S4V]-[V49A]-CXCL12-GPLS), (G) compound 6 ([S4V]-[V49A]-CXCL12), and (H) SBP. wt = wild type, SBP = surface-binding peptide, M_{av} = calculated average molecular weight, M_{mono} = calculated monoisotopic molecular weight, ACN = acetonitrile.

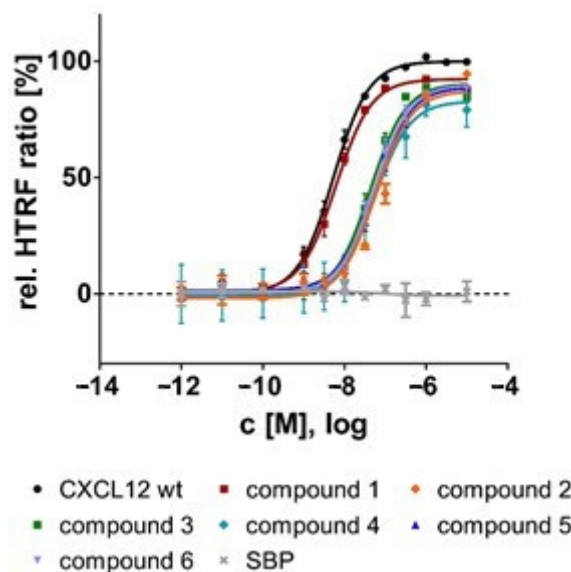


Figure S4. Activity of transiently transfected COS-7 cells with the CXCR4 and a chimeric G α_{qi} protein after stimulation with CXCL12 variants for 1 h. IP accumulation was detected by FRET-donor/acceptor-labeled antibodies and homogenous time resolved fluorescence (HTRF) was measured. Data was normalized to CXCL12 wt and is presented as mean \pm SEM, $n \geq 3$.

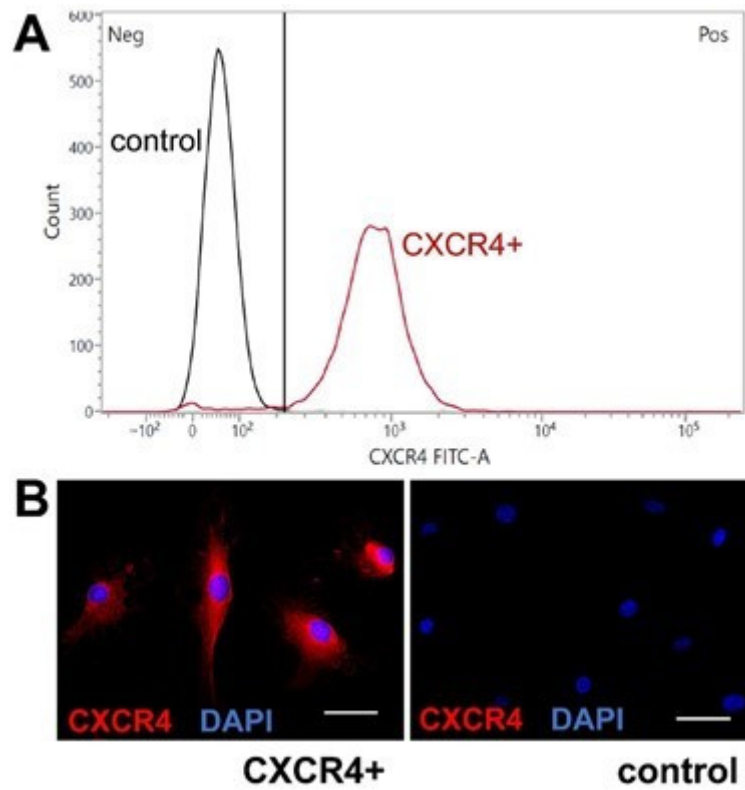


Figure S5. Characterization of murine MSCs. **(A)** FACS-CXCR4 staining. CXCR4 positive cells (primary murine MSCs) count from $CD45^{neg}/CD11b^{neg}/Sca1^{pos}/CD140a^{pos}$ cells; control w/o CXCR4-antibody. Cells were fixated with 4% paraformaldehyde and permeabilized with 0.1% saponin (in DPBS/Gelafusal®). **(B)** CXCR4 immune fluorescence staining. Cells were fixated with methanol and permeabilized with DPBS/ Tween 20.

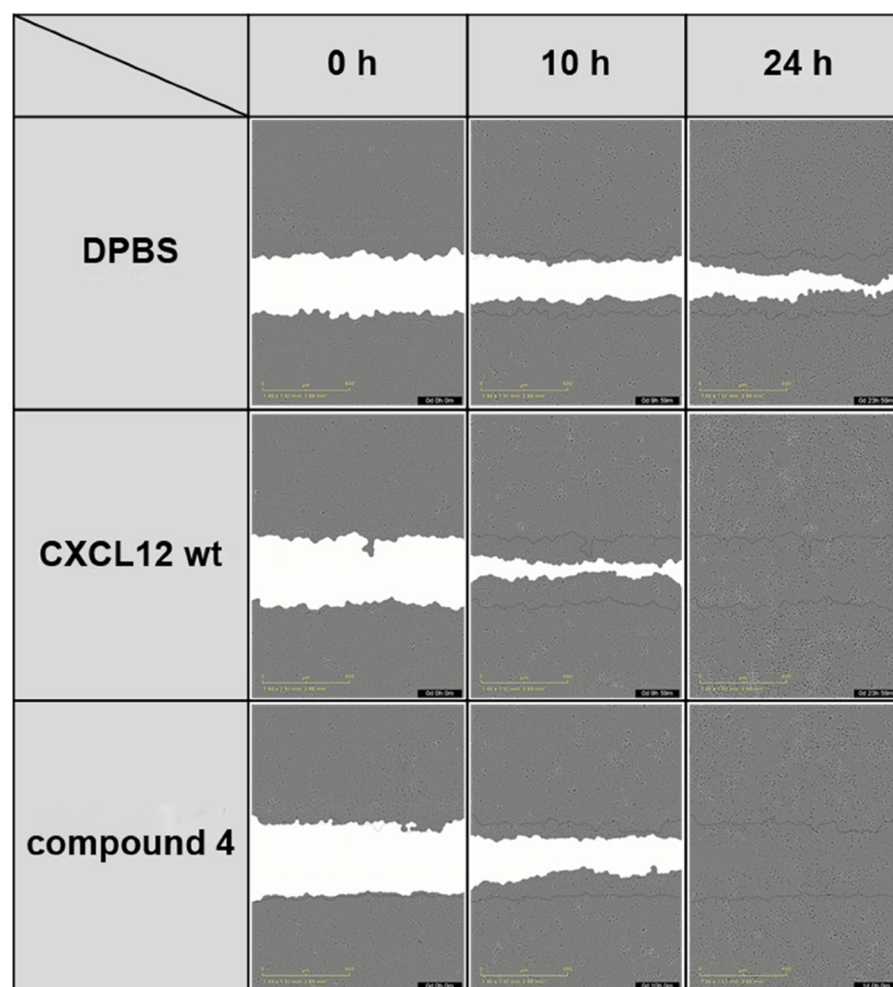


Figure S6. Representative pictures of gap closure after 0 h, 10 h, and 24 h by keratinocyte migration (HaCaT cells) in a scratch assay after pre-treatment with mitomycin C, a potent proliferation inhibitor. Cells were stimulated with 100 nM CXCL12 wt or compound 4.

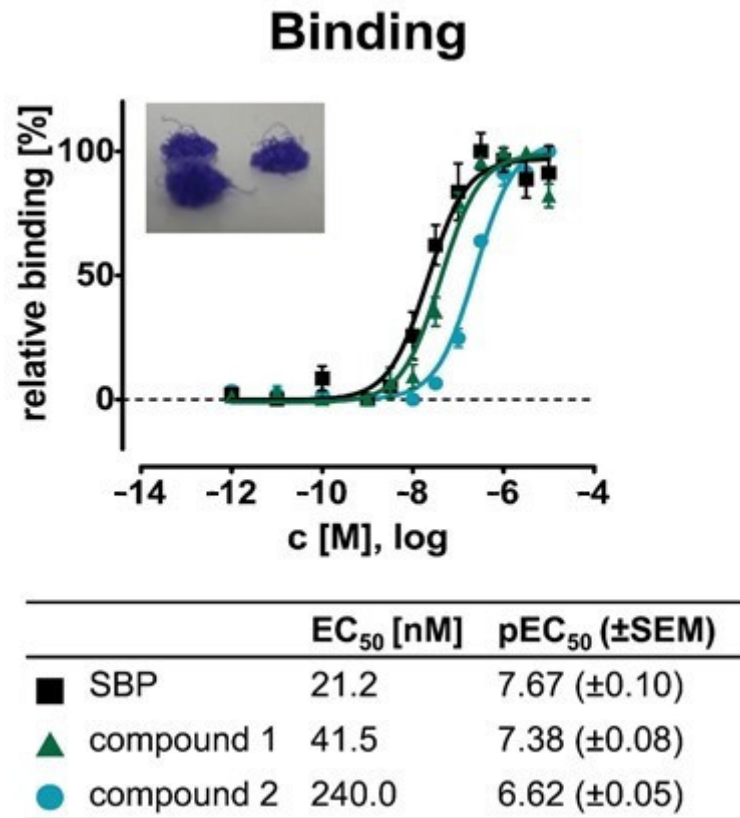


Figure S7. Binding affinities of indicated coatings shown on PCL-co-LC scaffolds in a concentration-dependent manner. Complete coating was achieved with 480 nM in case of compound 2. Data is presented as mean ± SEM, $n = 3$.

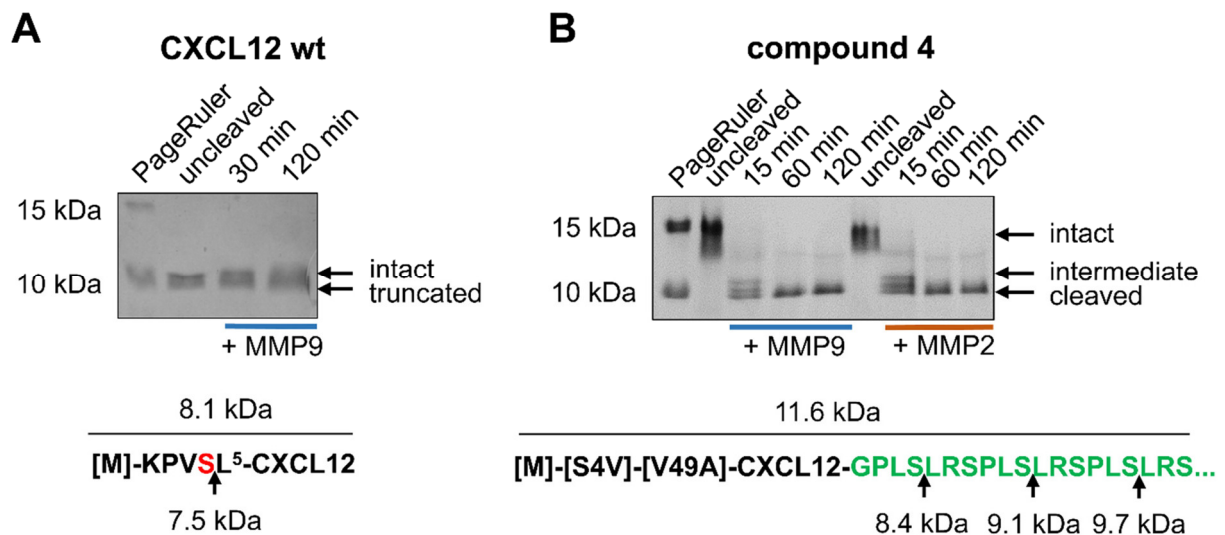


Figure S8. Stabilization and linker cleavage of modified CXCL12 in solution. (A) Truncation of native CXCL12 wt by MMP9 and (B) for the [S4V]-stabilized compound 4 with MMP9 and MMP2 (0.2 ng/μL), investigated by Tris/tricine SDS-PAGE. Corresponding cleavageproducts are indicated below.

A

human vs. porcine CXCL12

Range 1: 3 to 70 [Graphics](#) ▼ Next Match ▲ Previous Match

Score	Expect	Method	Identities	Positives	Gaps
142 bits(357)	3e-51	Compositional matrix adjust.	66/68(97%)	68/68(100%)	0/68(0%)

```

1  --KPVSLSYRCPCRFESHVARAIVCHLKILNTPNCALQIVARLNNNRQVCIDPKLKWIQEYLEKALNH----- 68
1  DEKPVSLSYRCPCRFESHVARAIVCHLKILNTPNCALQIVARLNNNRQVCIDPKLKWIQEYLEKALNHPSPTLSGLTS 80

81  ALGSSLASTTVGITSRS 97

```

B

human vs. porcine CXCR4

Range 1: 1 to 337 [Graphics](#) ▼ Next Match ▲ Previous Match

Score	Expect	Method	Identities	Positives	Gaps
655 bits(1691)	0.0	Compositional matrix adjust.	317/337(94%)	330/337(97%)	1/337(0%)

```

Query 1  MEGISITYSDNYTEE-MGSGDYDSMKPCFREANANFNKIFLPTIYSIIFLTGIVGNGLV 59
Sbjct 1  M+G I+TSDNYTE+ +GSGDYDS+KEPCFREENA+FN+IFLPT+YSIIFLTGIVGNGLV 60
MDGFRIFTSNYTEDDLGSGDYDSIKEPCFREENA+FN+IFLPTVYSIIFLTGIVGNGLV

Query 60  ILVMGYQKKLRSMTDKYRLHLSVADLLFVITLPFWAVDAVAMWYFGNFKAVHVIYTVN 119
Sbjct 61  ILVMGYQKKLRSMTDKYRLHLSVADLLFV+TLPFWAVDAVAMWYFG FLCKAVHVIYTVN 120
ILVMGYQKKLRSMTDKYRLHLSVADLLFVLTLPFWAVDAVAMWYFGKFLCKAVHVIYTVN

Query 120  LYSSVLILAFISLDRLAIVHATNSQRPRLKLAEKVVYVGVWIPALLLTIPDFIFANVSE 179
Sbjct 121  LYSSVLILAFISLDRLAIVHATNSQRPRLKLAEKVVYVGVWIPALLLTIPDFIFANV E 180
LYSSVLILAFISLDRLAIVHATNSQRPRLKLAEKVVYVGVWIPALLLTIPDFIFANVRE

Query 180  ADDRYICDRFYPNDLWVVFQFHIMVGLILPGIVILSCYCIISKLSHSGKHQRKALK 239
Sbjct 181  D RYICDRFYPNDLW+VVFQFHIMVGLILPGIVILSCYCIISKLSHSGK+QKRKALK 240
GDGRYICDRFYPNDLWVVFQFHIMVGLILPGIVILSCYCIISKLSHSGYQKRKALK

Query 240  TTVILILAFFACWLPYYIGISIDSFILLEIIKQGEFENTVHKWISITEALAFFHCCLNP 299
Sbjct 241  TTVILILAFFACWLPYYIGISIDSFILLEII+QGCEFE+TVHKWISITEALAFFHCCLNP 300
TTVILILAFFACWLPYYIGISIDSFILLEIIQGCEFE+TVHKWISITEALAFFHCCLNP

Query 300  ILYAFLGAKFKTSAQHALTSVSRGSSLKILSKGKRGG 336
Sbjct 301  ILYAFLGAKFKTSAQHALTSVSRGSSLKILSKGKRGG 337

```

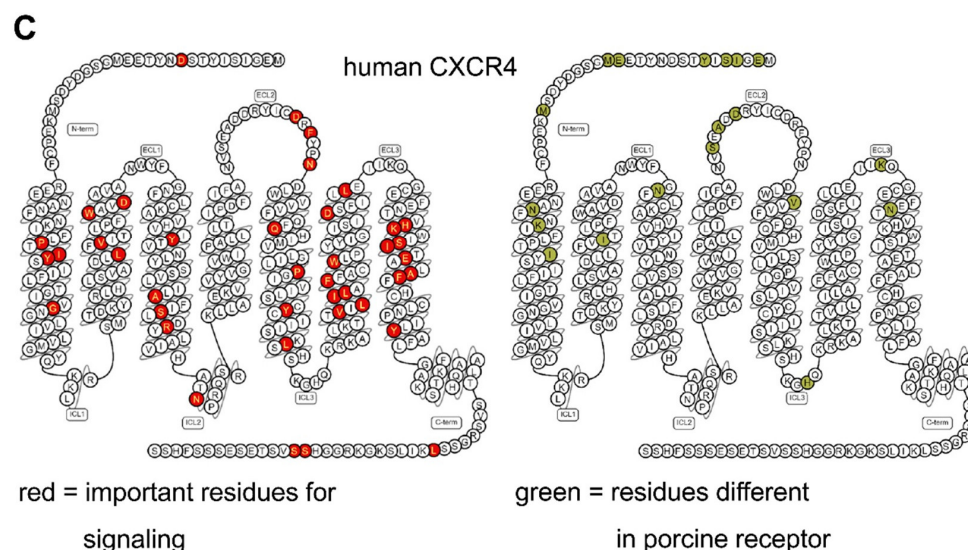


Figure S9. Sequence alignment (NCBI BLAST) of human and porcine CXCL12 and CXCR4. (A) Human vs. porcine mature CXCL12 show 97% sequence identity. Differences where highlighted in red boxes. (B) Human CXCR4 isoform 1 precursor vs. porcine CXCR4 precursor display 94% sequence identity. (C) Snake plot (GPCRdb) of human CXCR4, left: red dots indicate important residues for CXCR4/CXCL12 signaling found by Wescott et al. Proc Natl Acad Sci USA 2016) 9928-9933 [116]; right: green dots indicate residues which are different in porcine CXCR4. Only I44V in transmembrane helix 1 is overlapping important and different residue, but shares the same properties.